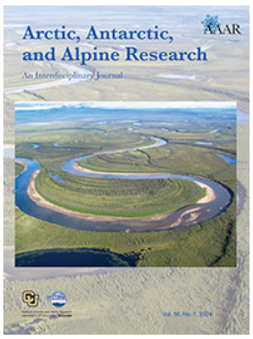

Taylor & Francis
Taylor & Francis Group

Arctic, Antarctic, and Alpine Research

An Interdisciplinary Journal

ISSN: 1523-0430 (Print) 1938-4246 (Online) Journal homepage: www.tandfonline.com/journals/uaar20

Measuring and modelling functional moat area in perennially ice-covered Lake Fryxell, Antarctica

Michael S. Stone, Mark R. Salvatore, Hilary A. Dugan, Madeline E. Myers & Peter T. Doran

To cite this article: Michael S. Stone, Mark R. Salvatore, Hilary A. Dugan, Madeline E. Myers & Peter T. Doran (2024) Measuring and modelling functional moat area in perennially ice-covered Lake Fryxell, Antarctica, Arctic, Antarctic, and Alpine Research, 56:1, 2406626, DOI: 10.1080/15230430.2024.2406626

To link to this article: https://doi.org/10.1080/15230430.2024.2406626

ARCTIC, ANTARCTIC, AND ALPINE RESEARCH
2024, VOL. 56, NO. 1, 2406626
https://doi.org/10.1080/15230430.2024.2406626

Taylor & Francis
Taylor & Francis Group

Measuring and modelling functional moat area in perennially ice-covered Lake Fryxell, Antarctica

Michael S. Stone [a], Mark R. Salvatore [b], Hilary A. Dugan [c], Madeline E. Myers [d], and Peter T. Doran [a]

[a]Department of Geology & Geophysics, Louisiana State University, Baton Rouge, Louisiana, USA; [b]Department of Astronomy and Planetary Science, Northern Arizona University, Flagstaff, Arizona, USA; [c]Center for Limnology, University of Wisconsin–Madison, Madison, Wisconsin, USA; [d]Department of Geography and Planning, Queen's University, Kingston, Ontario, Canada

ABSTRACT

The perennially ice-covered lakes of the McMurdo Dry Valleys (MDVs), Antarctica, are an important reservoir of liquid water in an arid and largely frozen environment. During the austral summer, the margins of these ice covers melt, forming a "moat" of liquid water and thin ice, allowing exchange between lake waters and the atmosphere to occur and serving as an interface between lake, soil, and stream ecosystems. The size of these moats varies from year to year. Here, we have established the first published record of moat area changes at MDVs' Lake Fryxell through time using manual traces of the moat as observed via satellite imagery. We have also tested a semi-automated approach for measuring moat area and found that it consistently underestimated the manual record, which we suspect may be due to the lower spatial resolution of images used in this versus the manual approach. Finally, we developed a predictive model based on readily available climate data, allowing moat area to be predicted beyond the limits of the satellite-based records. We found that functional moat area varies annually, potentially influencing ecosystem processes in the moats.

ARTICLE HISTORY
Received 9 April 2024
Revised 26 July 2024
Accepted 9 August 2024

KEYWORDS
McMurdo Dry Valleys; Lake Fryxell; moat; NDWI; predictive model; lake ice

Introduction

The McMurdo Dry Valleys (MDVs) of Antarctica are the largest relatively ice-free part of the continent (Figure 1; Levy 2013) and are home to more than 6,000 lakes and ponds (Hawes et al. 2021). The larger lakes generally boast a several meter thick, perennial ice cover, which helps to maintain the liquid state of the lakes (Doran, Wharton, and Lyons 1994). In the extreme polar desert ecosystem of the MDVs, where liquid water plays a critical role in supporting life and facilitating ecosystem connectivity across the landscape (Gooseff et al. 2011), these large lakes provide an important year-round stable reservoir of liquid water in an otherwise harsh and largely frozen environment.

Perennial lake ice covers limit exchanges between lake water and the atmosphere, prevent wind driven mixing, limit sedimentation and the amount of light penetration into the water column, and allow highly stratified water columns to persist (Doran, Wharton, and Lyons 1994; McKay et al. 1994; Spigel and Priscu 1998). For much of the year, these ice covers extend to the lakeshore, freezing to the underlying substrate and effectively sealing off the lake waters completely. However, during the austral spring and summer, the grounded ice melts and thins from the bottom up, in some places melting to the surface leading to the appearance of open water areas on and around the lake ice cover (Stone et al. 2024). These shallow lake regions that undergo seasonal freeze-thaw cycles are called "moats." While moats are generally restricted to a lake's perimeter, islands and shallow regions away from the lake shore can also lead to the development of moats toward the interior of ice-covered lakes.

Moats act as the interface between soil, stream, and lake ecosystems. The annual thawing and refreezing of moat ice creates a unique and challenging environment for the organisms residing there, and the benthic communities in the moats are taxonomically distinct from those in the deeper, perennially ice-covered parts of the lake (Stone et al. 2024). Many of the closed-basin lakes in

CONTACT Michael S. Stone mston26@lsu.edu Department of Geology & Geophysics, Louisiana State University, E235 Howe Russell Kniffen, Baton Rouge, Louisiana 70803, USA
Supplemental data for this article can be accessed online at https://doi.org/10.1080/15230430.2024.2406626

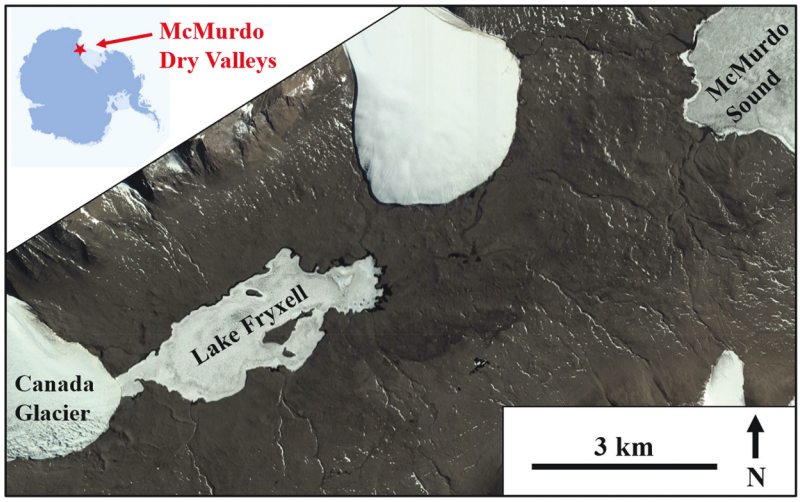

Figure 1. Location of Lake Fryxell within Taylor Valley. The dark region around Lake Fryxell's ice cover is the functional moat. Inset map shows the location of the McMurdo Dry Valleys in Antarctica. Base image from Google Earth Pro 7.3.6.9750 (January 17, 2010).

the MDVs are experiencing lake-level increases, and as they rise, lakeshore soil communities are inundated and incorporated into the moats (Ramoneda et al. 2021). Thus, moats can also provide an important catalyst driving ecological succession. When open water areas develop in the moats, they provide a conduit for exchange between the lake waters confined beneath the perennial lake ice cover and the atmosphere (Stone et al. 2024).

We define the functional moat of a lake as areas where liquid moat waters appear at the surface, or where waters are separated from the surface by a thin veneer of ice. This thin veneer of ice may melt and refreeze several times during a given season based on surface temperatures and is thin enough to allow light to pass through it without a notable decrease in transmission. The size of the functional moat has major implications for moat communities. Communities residing in open water moat areas receive much greater photosynthetically active radiation (PAR) than those residing beneath lake ice (Hawes and Schwarz 1999); thus the size of the functional moat controls the degree and spatial extent of PAR availability for lake marginal communities. Although evaporation is considered only a minor contributor to MDV lake volume loss and drawdown (Dugan, Obryk, and Doran 2013), the size of open water areas of the functional moat logically impacts lake evaporation rates and controls its influence on overall lake ablation. Evaporation may also contribute to the increases in solute concentrations through the austral summer observed in the moat waters (Stone et al. 2024), changing the chemistry of the waters in which moat communities reside. In addition, the area of the functional moat controls how much wind can influence the moat environment, with the greater fetch of larger moats being more subject wind-driven wave action and thus having more potential for higher turbidity.

Here, we define and compare means of tracking functional moat area from satellite imagery both manually and via a semi-automated method. In doing so, we establish the first published functional moat area record for Lake Fryxell, a perennially ice-covered, closed-basin lake located in eastern Taylor Valley (Figure 1). In addition, we develop a predictive model for Lake Fryxell functional moat area based on routinely measured climate variables collected at a nearby automated meteorological station. The goal of this model is to find a simple means of predicting functional moat area using readily available climate data, and to identify correlations between functional moat area and climate variables. The model facilitates hindcasting, providing a means to extend the functional moat area record beyond the temporal limits of the satellite imagery-based datasets, and filling in gaps in the functional moat area record.

Setting

Lake Fryxell [77°36' S, 162°6' E] is a closed-basin lake that lies at the eastern end of Taylor Valley, an east-west trending valley whose eastern margin opens to the McMurdo Sound region of the Ross Sea. The lake has an area of roughly 7 km^2 and is approximately 20 m deep. The perennial lake ice cover on Lake Fryxell has varied from 2.9 to 6.2 m over the monitoring record (Priscu 2003). The lake ice is highly weathered and opaque, and generally has a high albedo relative to moat ice. It has a mostly white appearance except where wind-blown sediment patches have accumulated

on the ice cover's surface, or surface melt has led to ponding followed by refreezing on the lake ice surface. Conversely, early spring and summer moat ice is smooth, largely transparent (especially where the ice is thinnest within the first few meters of the lakeshore), and often has a blue appearance. Both moat and perennial lake ice undergo whitening as the austral summer progresses, lowering their transmissivity (Fristen and Priscu 1999) and their optical reflectance.

Lake Fryxell's closed-basin means it is susceptible to lake level changes. A manual record of the lake's level has been maintained since 1972, and the lake has generally risen since the start of that record, ranging from 15.7 to 18.5 m above sea level (Barrett et al. 2008; Doran and Gooseff 2023). Lake level changes reflect the balance of water inflows minus evaporation and sublimation. Water inputs into the lake largely come from meltwater streams flowing into the lake from local alpine glaciers, or from direct melt discharged from Canada Glacier, which abuts the western end of the lake (Miller and Aiken 1996; McKnight et al. 1999). The extreme aridity of the MDVs means precipitation, almost exclusively in the form of snow, is limited to between 3 and 50 mm water equivalent per year (Fountain et al. 2009). While precipitation feeds the glaciers that feed the streams and ultimately the lakes, direct precipitation into the lakes is not considered to have any notable effect on MDV lake levels. As there are no surface outflows from Lake Fryxell, water loss from the lake is due to ablation of the lake ice cover and, likely less so, from evaporation of the open water moat (Doran, Wharton, and Lyons 1994; Dugan, Obryk, and Doran 2013). A groundwater system flowing beneath Lake Fryxell to the McMurdo Sound may also play a role in controlling lake level (Foley et al. 2019).

Average annual valley bottom air temperatures in Fryxell Basin, measured at the Lake Fryxell Meteorological Station (FRLM) [77°36′40" S, 163° 10′12" E], range between −23.0 and −17.2°C (Obryk et al. 2020). The valley experiences 24-hour daylight during the summer months, with solar radiation reaching the surface being impacted by diurnal and annual changes in the relative position of the sun, and atmospheric conditions including cloud cover. During the summer, Lake Fryxell generally experiences more overcast days than more western parts of the valley (Acosta, Doran, and Myers 2020).

Methods

Manual record

A manual functional moat area record was acquired via manual tracing of the functional moat regions of Lake Fryxell observed from satellite images. A single panchromatic (450–800 nm) satellite image from either the WorldView-2 (WV2; 46 cm pix^{-1} ground resolution) or −3 (WV3; 31 cm pix^{-1} ground resolution) satellites was selected from near the height of the austral summer each year with the goal of capturing the maximum extent of the functional moat for each season. The WV2 and WV3 satellites are in near-polar orbits, enabling rapid repeat measurements, although satellite tasking demands limit the frequency of image acquisition over Lake Fryxell. The georeferenced and georectified imagery used for this research was acquired through the National Science Foundation (NSF) Polar Geospatial Center at the University of Minnesota through a cooperative agreement with the National Geospatial Intelligence Agency. Satellite images were selected based on the following criteria: 1) the image contained Lake Fryxell in its entirety, 2) Lake Fryxell's margins and islands were not obscured by cloud cover or shading to a degree that functional moat areas were non-discernible, 3) both the shoreline and the transition between moat and permanent ice were easily discernible, and 4) the images were acquired on or after January 1st during the target austral summer, with preference going to the latest images acquired during a given summer that satisfied the other three criteria. Three additional images acquired prior to January 1st, corresponding to early season images selected for semi-automated functional moat classification (described below), were also selected for manual tracing. These early season manual traces, along with the rest of the manual dataset, were used to check the accuracy of the semi-automated classification methods.

Manual tracing of moat extent was performed in QGIS Desktop 3.26.2 using WGS84/Antarctic Polar Stereographic Coordinate Reference System by creating polygon shapefiles outlining the lake, the perennial lake ice cover, islands in the lake, and holes in the lake ice cover created by those islands or by recently submerged former islands (Figure 2). Where snowbanks obscured the shoreline, the lake-proximal edge of the snowbank was traced. In other cases where the margin of a feature being traced was unclear, the unclear margin was interpolated based on the nearest clear margins occurring before and after the unclear margin. Tracing was done at a 1:1000 scale using a 10 m by 10 m grid as a guide, with polygon vertices falling only on the gridlines to maintain an identical spatial resolution throughout. Polygon areas were calculated using the $area function of the Field Calculator tool, which calculates surface area with respect to the reference ellipsoid (WGS84) (QGIS Development Team 2024). The lake area for each image was calculated by subtracting the area of the islands

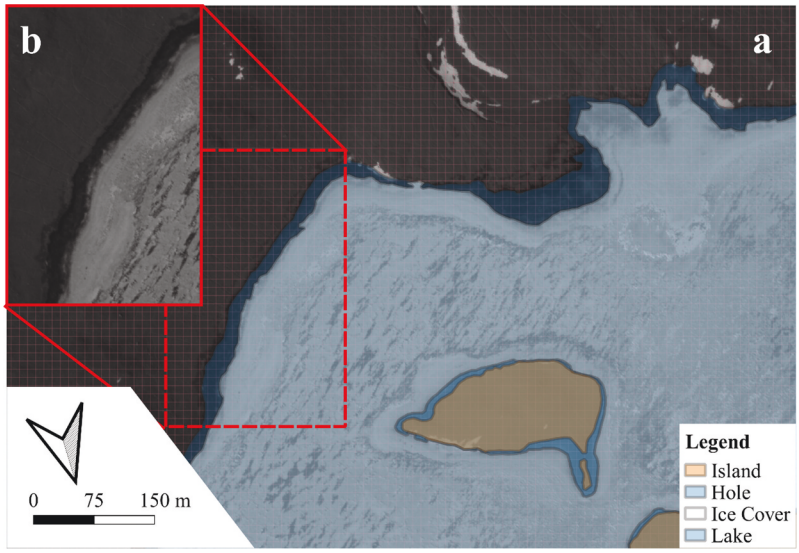

Figure 2. Image of a portion of Lake Fryxell a) with 10 m grid and manually traced polygons imposed and b) a portion of the base image displaying how the moat appears on the panchromatic imagery. Hole polygons denote the outlines of holes in the lake ice cover, and the lake polygon denotes the margin of the lake. The functional moat region is the area between the lake ice cover and the lakeshore, and the area between the lake ice cover and the islands. Imagery © 2019 Maxar.

from the area of the lake, and the ice cover area was calculated by subtracting the area of the ice cover from the area of the holes in the ice cover forming around islands. The functional moat area was calculated by subtracting the area of the ice cover from the area of the lake, and this was converted to a percentage of the total lake area (% TLA) to simplify inter-annual comparisons.

Semi-automated record

Our goal with establishing a semi-automated method for producing a functional moat area record was to find a simple, reliable, and easily reproducible approach that could quantify the area of open moat using extant and future imagery. Two semi-automated approaches were tested and compared with the manual functional moat area record: a Normalized Difference Water Index (NDWI)–based approach and a supervised classification approach. WV2 and WV3 8-band visible/near-infrared (VNIR; 0.43 μm – 0.91 μm) multispectral data were used for this study because of their combination of high spatial resolution (1.8–2.9 m pix^{-1}, depending on instrument, off-nadir pointing, and topography) and the ability to spectrally interrogate each pixel. All data were calibrated to surface reflectance using the methods of Salvatore et al. (2021, 2023), which utilizes five invariant ground control points surrounding Lake Fryxell. In order to minimize the inclusion of pixels not associated with the marginal lake moat, we limited our selection to only pixels within +2 and −4 vertical meters of the closest lake level measurement (Doran and Gooseff 2023) corresponding to each image's acquisition date using a digital elevation model (Fountain et al. 2017) and bathymetric contours (Doran, Wharton, and Schmok 1996). This method ensured that areas well outside of the moat region were excluded from our investigation, eliminating noise from shadows, sediment patches, and pools of meltwater found atop the perennial lake ice.

The semi-automated techniques used 11 images spanning January 2012 through December 2019 (Table S1). Three images were acquired during December, and the rest were acquired during January or February. A sequence of images was used for the 2014–15 and 2016–17 austral summers, and no images were classified from the 2010–11 or 2015–16 austral summers due to a lack of suitable images.

For the supervised classification approach, each image underwent a Minimum Distance supervised classification using endmembers aggregated from all the calibrated images used in this study (Table S2). Minimum Distance classification schemes assign each pixel to a specific class based on its "resemblance" in 8-band vector space to input endmember spectra, and has been successfully used to classify remote sensing data for more than half a century (e.g., Wacker and Landgrebe 1972). Classification endmembers included snow, rock/sediment, open water, blue ice, shadowed snow, shadowed rock/sediment, and mat-containing stream channels. Three different combinations of classified pixels were tested to determine which set of

endmembers best combine to match our manual moat record: the first used only pixels classified as open water; the second used a combination of open water, blue ice, and shadowed snow/ice pixels; and the third used the same combination as the second, but also included a reflectance threshold. Initial inspection revealed the open water only approach produced the best results, with a standard deviation of 0.95 percent TLA and a root mean square error (RMSE) of 2.19 percent TLA with respect to the manual record (Table S3).

The NDWI-based approach used a combination of NDWI (Gao 1996) and a threshold based on the 0.546 μm reflectance to identify pixels containing functional moat. NDWI was sensitive to the spectral "roll-off" imposed by water at near-infrared (NIR) wavelengths, while the albedo threshold helped to differentiate between ice, snow, and water. The NDWI of pixels were calculated using their green and NIR bands:

$$\frac{(Green - NIR)}{(Green + NIR)} = NDWI \quad (1)$$

Minimum threshold NDWI values for capturing the functional moat, all between 0 and 1, were tested by highlighting only pixels with NDWI values greater than those thresholds. The highlighted pixels were then visually compared with the green band image used in the NDWI calculation, in which the functional moat is readily apparent, to determine how well the highlighted pixels captured the functional moat. NDWI thresholds were systematically narrowed to find the value that best captured the true extent of the functional moat. This process was first performed on a single image, then the resultant NDWI threshold was tested on other images and adjusted as necessary to find the value best defining the functional moat in multiple images. The threshold value of >0.04 was determined to best identify pixels containing open water or water under a thin veneer of ice (i.e., functional moat). While this threshold value did a great job differentiating functional moat and the lake shore, it was less effective in differentiating functional moat from snow and ice (e.g., the permanent lake ice cover). For the albedo threshold, pixels with a reflectance value of <13 percent were identified as containing liquid water rather than snow or ice. This threshold value was determined by the same methods used for NDWI threshold determination. Combined, the NDWI and green band reflectance thresholds were found to uniquely identify the presence of liquid water with minimal confusion with nearby geological materials, snow, or ice.

Predicting functional moat area

To link moat extent to inter-annual differences in weather patterns, we used 15-minute data from FRLM that records air temperature at 3 m, wind speed, incoming solar radiation, and relative humidity since 1994 (Doran & Fountain 2023). We focused on climate variables that are routinely measured as part of the long-term record in order to allow for hindcasting and to make the model easily updatable for future functional moat area predictions. Different groupings of climate variables were tested in the model, with a focus on groupings of air temperature, solar radiation, and degree days as these have been shown to drive melt in the Dry Valleys (Doran et al. 2008; Hofsteenge et al. 2023). Specifically, we hypothesized that the same processes responsible for glacial melt in the Dry Valleys (i.e., temperature and insolation) were also responsible for moat development, and thus the number of warm and sunny days (*WSdays*) during an austral summer should be a good predictor of functional moat area that season. The number of degree days (*DD*) above a temperature threshold during a given season was also hypothesized to be a good predictor of functional moat area given the positive correlation between the number of DD above freezing with other MDV climate events, such as increases in streamflow and increases in strong, warming, down-valley foehn winds (Doran et al. 2008). DD refers to the cumulative number of days above a temperature threshold and was calculated by adding the above threshold portion of 15-minute average temperature measurements recorded at FRLM and dividing the sum by the number of temperature measurements recorded during each 24-hour span.

We built a simple model where moat extent was a function of the number of days when mean daily air temperature was above x_1 and mean daily solar radiation was above x_2. We applied a general-purpose optimization routine using the Nelder-Mead algorithm in R (R Core Team 2022) to minimize the r^2 of this function and determine the best parameters for x_1 and x_2. We then built a final linear regression model where moat extent was a function of the number of warm sunny days and DD. Moat extent was weighted by the number of observations each year. The final model was then used to hindcast moat extent prior to the remote sensing record.

Results

Manual record

The manual moat area record spans from the 2009–10 through the 2021–22 austral summers, with no data acquired during the 2015–16 and 2022–23 austral

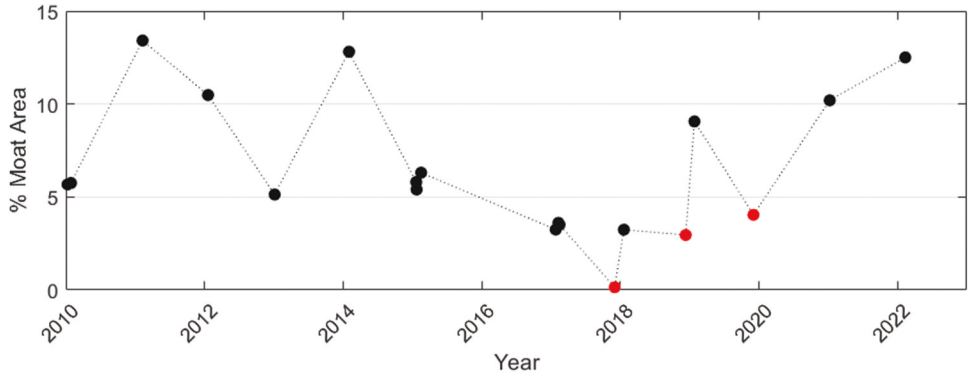

Figure 3. Manually derived percent functional moat area relative to the area of Lake Fryxell. Black points are from January or February. Red points are from December.

summers due to a lack of suitable imagery from those seasons (Figure 3, Table S1). In total, 19 images were used for this record, with 16 meeting all the listed criteria and the remaining three images being acquired prior to January 1 and corresponding to sample dates of the semi-automated record (Table S1). The largest percent functional moat areas captured in this record occurred on February 9, 2011 (13.4 percent TLA), February 1, 2014 (12.8 percent TLA), and February 10, 2022 (12.5 percent TLA). The smallest occurred on December 2, 2017 (0.1 percent TLA). However, the smallest functional moat captured after January 1st occurred on January 25, 2017 and January 19, 2018 (both 3.2% TLA). While the percent difference between large and small functional moat area years is substantial, direct comparison between data points is difficult as images were not acquired on the same day of the year each summer (image acquisition dates range between 2 December and 16 February) (Table S1).

Semi-automated record

The supervised classification and NDWI based approaches had similar results, yielding RMSEs of 2.19 percent TLA and 1.96 percent TLA, and standard deviations of 0.95 percent TLA and 0.87 percent TLA, respectively, relative to the manual measurements (Table S3). Both semi-automated methods resulted in functional moat area estimates that were consistently below the measurements of the manual record, with differences ranging from −0.1 percent TLA to −3.3 percent TLA in both approaches (Figure 4, Table S1). Thus, both methods generally underpredict functional moat area relative to the manual record, meaning they provide a lower limit estimate for functional moat area. For both approaches, we found no correlation between the amount of error and the manually measured area of the functional moat (Figure S1).

Using the results from three randomly selected images from each semi-automated technique, shapefiles containing moat and non-moat classified pixels within

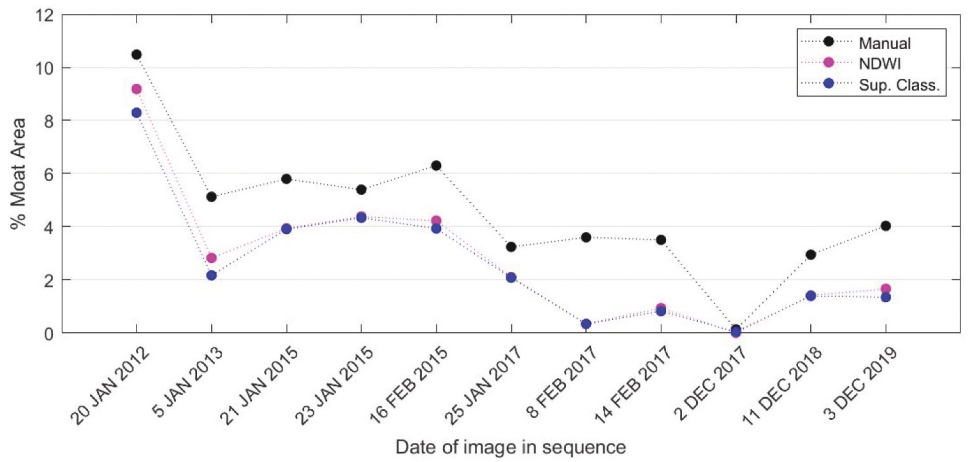

Figure 4. Percent functional moat area relative to the total lake area for sampled dates derived via manual tracing (black), the NDWI-based semi-automated approach (magenta), and the supervised classification approach (blue).

the target area as identified by each technique were directly compared to moat and non-moat shapefiles produced via manual tracing to further investigate underpredicting by those techniques. Thus, 95.2 percent of areas identified as containing moat via supervised classification, and 92.8 percent of those areas identified via the NDWI approach, corresponded to moat areas identified via manual tracing (Table S4); 96.5 percent of non-moat areas identified by both semi-automated approaches corresponded to non-moat areas identified by manual tracing, though supervised classification produced a lower standard deviation (± 1.5 percent) than the NDWI approach (± 1.9 percent) in this regard. Confusion matrices built from the three randomly selected results of each semi-automated technique reveal that in both methods, false negatives (i.e., predicted as non-moat but manually measured as moat) are more common than false positives (i.e., predicted as moat but manually measured as non-moat), leading to underestimation of the results (Table S5).

Predictive model

WSdays were calculated as the number of days each year when mean daily air temperature was greater than −1.5°C (x_1 = −1.5°C) and mean daily incoming shortwave radiation was greater than 367 W m^{-2} (x_2 = 367 W m^{-2}). *WSdays* ranged from a low of three prior to Dec 11th, 2018, to a high of nineteen prior to Feb 1st, 2014. From 1994 to 2022, Jan 18th was the maximum day these conditions were met. DD above 3°C further improved model fit (DD_3 range = 0 to 5.37). Our final linear model to predict manual functional moat area data was (Figure 5):

$$Moat\ percentage = (0.533 * WSdays) + (0.652 * DD\_3^{\circ}C) + 1.66 \quad (2)$$

The adjusted R-squared fit of the model was 0.87, and all parameters were significant ($p < 0.05$). Applying our model to historic climate data from 1994 to 2022, predicted moat extent on Jan 31st ranged from 2.24 percent TLA in 2000–2001 to 21.3 percent TLA in 2001–2002 (Figure 6). Only 2001–2002, a particularly high melt season in the MDVs (Doran et al. 2008), fell outside the bounds of observation data on which the model was constructed.

Discussion

The manually derived functional moat area record provided the highest level of human oversight of the methods used in this study. However, this method does provide room for inconsistency between and among individuals doing the manual tracing and other forms of human error. Despite this, the protocols mentioned in the methods for manual tracing were intended to minimize human error as much as possible, and the same individual was used for all manual traces to keep things as consistent as possible. We thus considered the manual functional moat area record to be our standard for measuring functional moat area on each of the measurement dates.

Drawbacks of the manual record included the time investment (>3 h per complete trace) and the possible lack of reproducibility (*i.e.* it is possible that new individuals contributing to the manual record will introduce new error despite the protocols outlined in this manuscript). The semi-automated approaches addressed both drawbacks by providing fixed parameters that could

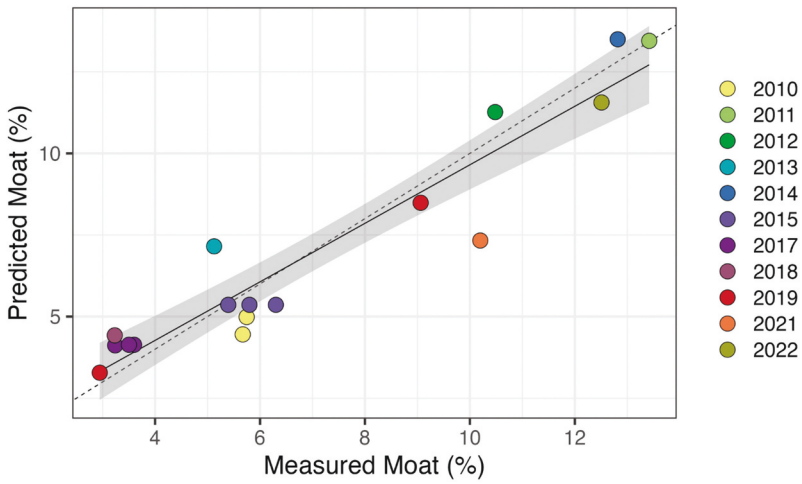

Figure 5. Manually measured percent functional moat area relative to the total lake area versus the predicted percent functional moat area. Line of best fit was drawn for data including (solid line) and without (dashed line) the 2021 datapoint.

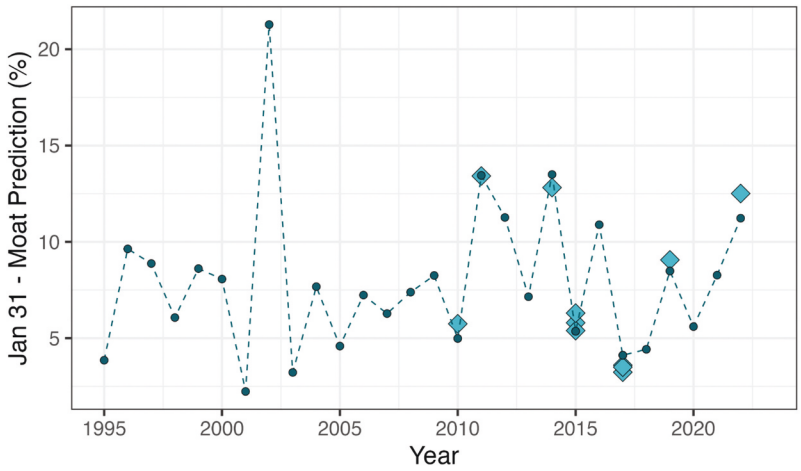

Figure 6. Model predicted percent functional moat area relative to the total lake area for January 31 each year, extended beyond the limits of the manual record using the historic air temperature and solar radiation data. Light blue diamonds represent the manually derived functional moat area between January 21 and January 31.

rapidly be applied to images of Lake Fryxell to estimate moat area, provided those images contained the appropriate wavelengths, were atmospherically corrected and calibrated to surface reflectance, and met the other image requirements described in the methods section of this manuscript. Thus, the semi-automated approaches may be better than the manual approach for maintaining a functional moat area record long-term and through changing hands.

Results of the NDWI and supervised classification based semi-automated approaches were similar, though the NDWI approach resulted in a slightly higher RMSE and standard deviation than the supervised classification approach (Table S3). However, the NDWI approach produced more false positive moat identifications than supervised classification (Table S4). Given that both techniques consistently underestimated the manually measured functional moat area, it seems likely the higher prevalence of false positives in the NDWI approach are responsible for the higher RMSE resulting from that method. Thus, it does not make sense to declare the NDWI approach the better of the 2 techniques. Given the similarity in their results, we suggest both approaches are viable options for estimating functional moat area.

The semi-automated approaches consistently underestimated manually measured functional moat areas. The degree of this underestimation did not show any correlation with changes in functional moat area (Figure S1), and thus it seems unlikely that the estimated functional moat area is notably influenced the number of moat-containing pixels identified in a sample image. This suggests that although false negative moat identifications are common relative to false positives (Table S5), the occurrence of false negatives does not compound with increasing moat area.

The consistency of the underestimated moat area estimates produced by the semi-automated techniques (e.g., Figure 4, Table S3) may be due to the lower spatial resolution multispectral imagery used for spectral remote sensing as opposed to the ~2x higher spatial resolution panchromatic imagery used for the manual dataset. We hypothesized that the apparent lower RMSE limit at ~2 percent, observed in the results of both methods (Table S3), would become smaller if higher spatial resolution multispectral imagery were used in the future, or, conversely, if the same resolution imagery were used for both the manual and semi-automated methods. Field-based ground truthing in future years is also expected to help improve the accuracy of the semi-automated techniques.

Although functional moats were small during the early part of the season and the largest moat areas all occurred during the month of February, the date of a measurement alone did not appear to be a good predictor of functional moat area. In the manual record, moats as small as 3.5 percent TLA were observed in February, and moats as large as 10.2 percent TLA were seen in the first half of January (Figure 3).

Our predictive model generally did a good job of predicting functional moat area as measured by the manual record, indicating a strong correlation between temperature, shortwave radiation, and functional moat area. The model's largest outliers were the January 8, 2021 and January 5, 2013 predictions, with differences between predicted and measured moat areas of 2.87 percent TLA and −2.02 percent TLA, respectively (Figure 5, Table S6). While the cause of these relatively larger

outlier predictions are not known, they are the two earliest January predictions in our record. It is possible that thermal inertia plays a larger role in the later season moat areas, thus resulting in an offset in our early January predictions. Accounting for this would require a more dynamic model beyond the scope of this manuscript and would likely require us to abandon our goal of creating a predictive model using only readily available climate data.

Since the model relied solely on long-term meteorological data from FRLM, which has been in operation since 1994, the model could be used for hindcasting. This allowed us to predict the percent size of the functional moat during years when no usable satellite imagery existed, especially in the months of January and February when functional moats tended to be at their largest. Hindcasting required the specification of a date to predict the corresponding functional moat area. We arbitrarily selected January 31st each year for our model predictions (Figure 6). The predicted large moat area in 2002 corresponded to the year of the greatest amount of streamflow and lake level rise on record in the McMurdo Dry Valleys, known as the "flood year" (Doran et al. 2008). The large predicted functional moat area in 2002 is related to the 2001–2002 austral summer having, by far, the highest number of DD above 3°C compared to any other season measured (Fig. S2). While five of the six largest moats were predicted to have occurred since 2011, there was no statistical difference in the mean moat size between 1995–2010 (excluding 2002) and 2011 to 2022 (t-test, $p = 0.5$). The increased variation in moat size may have been related to other recent landscape changes in the region (e.g., increases in glacial ablation, stream erosion, and landscape lowering via deflation), which are attributed to increasing solar radiation from anthropogenic climate change (Fountain et al. 2014). If true, given the correlation between functional moat area and both solar radiation and temperature, we suspect functional moat area will continue to increase as the regional climate warms in the coming decades (e.g., Shindell and Schmidt 2004; Arblaster and Meehl 2005; Chapman and Walsh 2006).

Our functional moat area records showed the percent functional moat area changing from year to year (Figures 3, 4 and 6). This suggests that the moat environment is subjected to varying levels of light, wind driven mixing and turbidity, and evaporation annually, adding to the environmental stresses moat communities are subjected to. Evaporation is generally considered to play only a minor role in total water mass loss in MDV lakes (Dugan, Obryk, and Doran 2013). However, we measured functional moat areas as large as 13.4 percent TLA. As evaporation requires far less energy than sublimation, this may imply that during large functional moat years, evaporation from the moats can be a major contributor to lake volume loss. Thus, functional moat area may play an important role in controlling lake water balance. The correlation between warm and sunny days and functional moat area further suggests that during large functional moat years, not only are moat communities subject to greater amounts of PAR due to a thin or missing moat ice cover, they also are receiving greater amounts of PAR due to the meteorological conditions of that season. The reverse appears to be true during small functional moat years, with moat communities receiving less PAR due to both a more persistent and thicker moat ice cover, and due to a lower number of warm and sunny days. Thus, functional moat area may play an important role in influencing ecosystem processes in the moat environment annually.

Moats represent an important landscape unit within the MDVs, acting as a dynamic interface between terrestrial and aquatic ecosystems (Stone et al. 2024). Indeed, their seasonally ice-free nature may provide the first glimpse into the future of MDV lakes, which are predicted to lose their perennial ice covers within the next few decades (Obryk, Doran, and Priscu 2019). Thus, understanding the moat environment is essential for understanding the present and future ecology of MDV lakes and how they connect to the broader MDV environment. Although this study focused largely on annual changes in functional moat area at Lake Fryxell, our methods can be easily adapted to other MDV water bodies and to investigate seasonal trends in functional moat growth, provided the appropriate satellite imagery becomes available. This study also paves the way for future research into the spatial components of functional moat development (e.g., what causes some regions of a lake to develop wide moats while other areas have little to no moat?). It is our hope that future additions to this dataset will be complimented by field-based ground truthing to allow us to fine tune our methodology and further improve this important new dataset.

Conclusions

When the protocols we have outlined in the methods were adhered to, manual functional moat area tracing provided the most reliable means of measuring functional moat area on satellite imagery. However, the manual method was more subject to human error and required much more time than semi-automated methods. The two semi-automated approaches did a suitable job of estimating moat area and could be readily applied to future satellite imagery to help maintain the functional moat record over the long term. These approaches

were not subject to the same level of human error that the manual approach was as they were minimally dependent on human interpretation. Still, some human interpretation-based input was necessary in both methods, with threshold values for both the NDWI and albedo parameters having been selected manually. Despite reducing human error, the semi-automated approaches did present some possible shortcomings, namely that they consistently underpredicted functional moat area compared to the manual record. This underpredicting may have been a product of the lower spatial resolution of the satellite imagery used in the semi-automated approaches relative to the manual approach. We therefore recommend that functional moat areas derived via either of the semi-automated approaches be treated as low-end estimates, being likely smaller than the true extent of the functional moat.

Our climate-variable based model was effective in predicting functional moat area in most cases and provided a means of hindcasting functional moat area beyond the limits of our satellite imagery-based records. The reliance of the predictive model on routinely measured meteorological variables meant it could be rapidly and easily applied. The availability of satellite imagery was dependent on several factors, including atmospheric conditions, shading, and satellite tasking demand. Thus, our predictive model provided a means of filling in gaps in the functional moat area record.

Functional moat area varied from year to year, likely controlling the degree of meteorological influences on the moats and the communities they contain. Large functional moats likely lead to greater amounts of evaporation, and the annual variance in functional moat area may play an important role in controlling total lake water balance. This variance may also help control annual PAR availability for organisms residing in the moat, thus influencing moat ecosystem processes.

Disclosure statement

No potential conflict of interest was reported by the author(s).

Funding

This work was supported by the National Science Foundation, Grant #OPP-1637708, for Long Term Ecological Research (LTER) and the John Franks Fund at Louisiana State University.

ORCID

Michael S. Stone http://orcid.org/0000-0002-1069-016X
Mark R. Salvatore http://orcid.org/0000-0002-1551-8342
Hilary A. Dugan http://orcid.org/0000-0003-4674-1149
Madeline E. Myers http://orcid.org/0000-0002-2431-5520
Peter T. Doran http://orcid.org/0000-0002-3774-2847

Author contributions

MSS, MEM, & PTD came up with the concept for this article, and all authors contributed to developing that concept. MEM created an original (non-standardized) manual traces and predictive model that inspired this work. MSS & MRS wrote the methods for the semi-automated classification. HAD wrote the methods and results for the predictive model, and designed the model used in this work and created Figure 5 and 6. MSS wrote the initial draft of the remaining parts of the manuscript, created the manual traces, refined the NDWI-approach's parameters, and created Figure 1–4 and S1 and Tables S1–S5. MRS conceived and conducted the analysis for all the semi-automated approaches mentioned. All authors contributed to editing this manuscript. Geospatial support for this work provided by the Polar Geospatial Center under NSF-OPP awards 1043681, 1559691, and 2129685.

References

Acosta, D., P. T. Doran, and M. Myers. 2020. GIS tool to predict photosynthetically active radiation in a Dry Valley. *Antarctic Science* 32, no. 5: 315–28. doi:10.1017/S0954102020000218.

Arblaster, J. M., and G. A. Meehl. 2005. Contributions of external forcings to southern annular mode trends. *Journal of Climate* 19, no. 12: 2896–2905. doi:10.1175/JCLI3774.1.

Barrett, J. E., R. A. Virginia, D. H. Wall, P. T. Doran, A. G. Fountain, K. A. Welch, and W. B. Lyons. 2008. Persistent effects of a discrete warming event on a polar desert ecosystem. *Global Change Biology* 14, no. 10: 2249–61. doi:10.1111/j.1365-2486.2008.01641.x.

Chapman, W. L., and J. E. Walsh. 2006. A synthesis of Antarctic temperatures. *Journal of Climate* 20, no. 16: 4096–4117. doi:10.1175/JCLI4236.1.

Doran, P., and A. Fountain. 2023. High frequency measurements from Lake Fryxell Meteorological Station (FRLM), McMurdo Dry Valleys, Antarctica (1993–2022, ongoing). *Environmental Data Initiative*. https://amrdcdata.ssec.wisc.edu/dataset/high-frequency-measurements-from-lake-fryxell-meteorological-station-frlm-mcmurdo.

Doran, P. T., and M. N. Gooseff. 2023. Lake level surveys in the McMurdo Dry Valleys, Antarctica (1991–2023, ongoing). *Environmental Data Initiative*. doi:10.6073/pasta/927439563d37c9461011e0060a5c1a87.

Doran, P. T., C. P. McKay, A. G. Fountain, T. Nylen, D. M. McKnight, C. Jaros, and J. E. Barrett. 2008. Hydrologic response to extreme warm and cold summers in the McMurdo Dry Valleys, East Antarctica. *Antarctic Science* 20, no. 5: 499–529. doi:10.1017/S0954102008001272.

Doran, P. T., R. A. Wharton Jr., and W. B. Lyons. 1994. Paleolimnology of the McMurdo Dry Valleys, Antarctica. *Journal of Paleolimnology* 10: 85–114.

Doran, P. T., R. A. Wharton Jr., and J. P. Schmok. 1996. Geophysical determination of bathymetry and morphology

of Taylor Valley lakes. *Antarctic Journal of the United States* 31: 198–200.

Dugan, H. A., M. K. Obryk, and P. T. Doran. 2013. Lake ice ablation rates from permanently ice-covered Antarctic lakes. *Journal of Glaciology* 59, no. 215: 491–498. doi:10.3189/2013JoG12J080.

Foley, N., S. Tulaczyk, D. Grombacher, P. T. Doran, J. Mikucki, K. Myers, N. Foged, et al. 2019. Evidence for pathways of concentrated submarine groundwater discharge in East Antarctica from helicopter-borne electrical resistivity measurements. *Hydrology* 6, no. 2: 54. doi:10.3390/hydrology6020054.

Fountain, A. G., J. C. Fernandez-Diaz, M. K. Obryk, J. Levy, M. N. Gooseff, D. J. Van Horn, P. Morin, et al. 2017. High-resolution elevation mapping of the McMurdo Dry Valleys, Antarctica, and surrounding regions. *Earth Systems Science Data* 9, no. 2: 435–443. doi:10.5194/essd-9-435-2017.

Fountain, A. G., J. S. Levy, M. N. Gooseff, and D. Van Horn. 2014. The McMurdo Dry Valleys: A landscape on the threshold of change. *Geomorphology* 225: 25–35. doi:10.1016/j.geomorph.2014.03.044.

Fountain, A. G., T. H. Nylen, A. Monaghan, H. J. Basagic, and D. Bromwich. 2009. Snow in the McMurdo Dry Valleys, Antarctica. *International Journal of Climatology* 30, no. 5: 633–642. doi:10.1002/joc.1933.

Fristen, C. H., and J. C. Priscu. 1999. Seasonal change in the optical properties of the permanent ice cover on Lake Bonney, Antarctica: Consequences for lake productivity and phytoplankton dynamics. *Limnology and Oceanography* 44: 447–54.

Gao, B.-C. 1996. NDWI - A normalized difference water index for remote sensing of vegetation liquid water from space. *Remote Sensing of the Environment* 58: 257–66.

Gooseff, M. N., D. M. McKnight, P. Doran, A. G. Fountain, and W. B. Lyons. 2011. Hydrological connectivity of the landscape of the McMurdo Dry Valleys, Antarctica. *Geography Compass* 5, no. 9: 666–681. doi:10.1111/j.1749-8198.2011.00445.x.

Hawes, I., C. Howard-Williams, N. A. Gilbert, and K. Joy. 2021. Towards an environmental classification of lentic aquatic ecosystems in the McMurdo Dry Valleys, Antarctica. *Environmental Management* 67: 600–622. doi:10.1007/s00267-021-01438-1.

Hawes, I., and A.-M. Schwarz. 1999. Photosynthesis in an extreme shade habitat: Benthic microbial mats from Lake Hoare, Antarctica. *Journal of Phycology* 35, no. 3: 448–459. doi:10.1046/j.1529-8817.1999.3530448.x.

Hofsteenge, M. G., N. J. Cullen, J. P. Conway, C. H. Reijmer, M. R. van den Broeke, and M. Katurji. 2023. Meteorological drivers of melt at two nearby glaciers in the McMurdo Dry Valleys of Antarctica. *Journal of Glaciology*. doi:10.1017/jog.2023.98.

Levy, J. 2013. How big are the McMurdo Dry Valleys? Estimating ice-free area using Landsat image data. *Antarctic Science* 25: 119–20.

McKay, C. P., G. D. Clow, D. T. Anderson, and R. A. Wharton Jr. 1994. Light transmission and reflection in perennially ice-covered Lake Hoare, Antarctica. *Journal of Geophysical Research* 99, no. 20: 427–20,444.

McKnight, D. M., D. K. Niyogi, A. S. Alger, A. Bomblies, P. A. Conovitz, and C. M. Tate. 1999. Dry valley streams in Antarctica: Ecosystems waiting for water. *Bioscience* 49, no. 12: 985–995. doi:10.1525/bisi.1999.49.12.985.

Miller, L. G., and G. R. Aiken. 1996. Effects of glacial meltwater inflows and moat freezing on mixing in an ice-covered Antarctic lake as interpreted from stable isotope and tritium distributions. *Limnology and Oceanography* 41, no. 5: 966–976. doi:10.4319/lo.1996.41.5.0966.

Obryk, M. J., P. T. Doran, A. G. Fountain, M. Myers, and C. P. McKay. 2020. Climate from the McMurdo Dry Valleys, Antarctica, 1986–2017: Surface air temperature trends and redefined summer season. *Journal of Geophysical Research: Atmospheres* 125, no. 13: e2019JD032180. doi:10.1029/2019JD032180.

Obryk, M. J., P. T. Doran, and J. C. Priscu. 2019. Predictions of ice-free conditions for a perennially ice-covered Antarctic lake. *Journal of Geophysical Research: Earth Science* 124, no. 2: 686–694. doi:10.1029/2018JF004756.

Priscu, J. 2023. Lake ice thickness and density measurements, McMurdo Dry Valleys, Antarctica (1989–2023, ongoing) [dataset]. *Environmental Data Initiative*. Accessed February 12, 2024. 10.6073/pasta/515c54434ee203a7611ed7db1e2501ae.

QGIS Development Team. 2024. QGIS 3.28 geographic information system user guide. *Open source geospatial foundation project*. https://docs.qgis.org/3.28/en/docs/user_manual/ .

Ramoneda, J., I. Hawes, A. Pascual-García, T. J. Mackey, D. Y. Sumner, and A. D. Jungblut. 2021. Habitat connectivity and environmental controls on the structure of phototrophic microbial mats and bacterioplankton communities in an Antarctic freshwater system. *FEMS Microbial Ecology* 97, no. 4: fiab044. doi:10.1093/femsec/fiab044.

R Core Team. 2022. *R: A language and environment for statistical computing*. Vienna, Austria: R Foundation for Statistical Computing. https://www.R-project.org/.

Salvatore, M. R., J. E. Barrett, S. R. Borges, S. N. Power, L. F. Stanish, E. R. Sokol, and M. N. Gooseff. 2021. Counting carbon: Quantifying biomass in the McMurdo Dry Valleys through orbital & field observations. *International Journal of Remote Sensing* 42, no. 22: 8597–8623. doi:10.1080/01431161.2021.1981559.

Salvatore, M. R., J. E. Barrett, L. E. Fackrell, E. R. Sokol, J. S. Levy, L. C. Kuentz, M. N. Gooseff, et al. 2023. The distribution of surface soil moisture over space and time in eastern Taylor Valley, Antarctica. *Remote Sensing* 15, no. 12: 3170. doi:10.3390/rs15123170.

Shindell, D. T., and G. A. Schmidt. 2004. Southern Hemisphere climate response to ozone changes and greenhouse gas increases. *Geophysical Research Letters: Climate* 31, no. 18. doi:10.1029/2004GL020724.

Spigel, R. H., and J. C. Priscu. 1998. Physical limnology of the McMurdo Dry Valley lakes. In *Ecosystem dynamics in a Polar Desert: The McMurdo Dry Valleys, Antarctica*, ed. J. C. Priscu, Antarctic Research Series, Vol. 72, 153–87. Washington, DC: American Geophysical Union.

Stone, M. S., S. P. Devlin, I. Hawes, K. A. Welch, M. N. Gooseff, C. Takacs-Vesbach, R. Morgan-Kiss, et al. 2024. McMurdo Dry Valley lake edge "moats": The ecological intersection between terrestrial and aquatic polar desert habitats *Antarctic Science*: 1–17. doi:10.1017/S0954102024000087.

Wacker, A. G., and D. A. Landgrebe. 1972. Minimum distance classification in remote sensing. *LARS Technical Reports*. Paper 25.